Microchemical and Microstructural Comparison of High Performance Nb_3Al Composites

P. J. Lee, A. A. Squitieri, D. C. Larbalestier, T. Takeuchi, N. Banno, T. Fukuzaki, and H. Wada

***Abstract*—We have performed a comparison of the microstructures of state of the art Nb_3Al composites processed using both ordinary RHQT (rapid-heating, quenching and transformation) and TRUQ (transformation-heat-based up-quenching) routes. Cross-sections were examined in the as-quenched, untransformed, and final size strands including Cu-clad strand. Both grain size and microchemistry were examined using a high resolution FESEM in BEI mode, using low accelerating voltage for grain orientation contrast and high voltage for atomic number contrast. The grain size is relatively large in these composites with a Feret diameter of 1300 nm for the TRUQ processed strand (compared with 70 to 160 nm for Nb_3Sn composites). In the untransformed strand electron backscatter indicated residual chemical inhomogeneity associated with the jelly-roll precursor. In the final strands the variations were much less but longitudinal cross-sections revealed the residual chemical inhomogeneity extending along the strand length. In both the ordinary and TRUQ (Cu and Cu-clad) processed strands a 1 μm thick 2-phase reaction layer was revealed on the outside surface of the outer filaments that had an average composition of 10% Al and 90% Nb. D.C. Magnetization measurements at 12 K indicated a 1 T improvement in irreversibility field, H^*, for the TRUQ strand compared with ordinary RHQT strands.**

***Index Terms*—Microstructure, Nb_3Al, strand, superconducting materials.**

I. Introduction

SIGNIFICANT advances have been made in recent years in the development of multifilamentary Nb_3Al for high field application. At magnetic fields above 20 T critical current densities can be obtained that are comparable to the best Nb_3Sn strands and useful critical current densities ($>$100 A/mm^2 nonstabilizer) can be achieved above 24 T. Furthermore the high strain tolerance of the Nb_3Al strands compared to Nb_3Sn is retained. The most successful strand fabrication techniques are based around high temperature heat treatments and rapid cooling. In the RHQT [1]–[3] process Nb/Al composites (modified jelly roll, MJR or rod in tube, RIT) are resistance heated to $\sim$1900 °C and then rapidly quenched into a molten Ga bath at $\sim$50 °C producing a metastable bcc supersaturated solid solution, $Nb(Al)_{ss}$, inside a Nb matrix. The $Nb(Al)_{ss}$ is then transformed to Nb_3Al at 800 °C. Both the critical temperature, T_c, and the critical magnetic field, B_{c2}, are lower for RHQT composites than the highest values obtained by laser or electron beam irradiation processed Nb_3Al and this difference has been attributed [4] to stacking faults formed in the A15 phase [5], [6]. Two successful modifications to the basic RHQT technique specifically address the stacking fault issue: In the double rapidly-heating/quenching, DRHQ, technique the standard RHQT process is followed but instead of a conventional low temperature ($<$1000 °C) transformation heat treatment a second RQH process produces the A15 phase and this is followed by a long range ordering heat treatment at 800 °C for $\sim$12 hrs (7). The T_c for these stacking fault free strands has been measured at 18.4 K, which suggests very good stoichiometry; furthermore a critical current density of 135 A/mm^2 was obtained at 25 T [4]. A disadvantage of this technique is that the brittle A15 phase is formed during high temperature processing. Alternatively the TRUQ technique (TRansformation-heat-based Up Quenching) [8] follows the initial RHQ of the RHQT process with a short heating step to 1000 °C, at 1000 °C the heat released by local transformation from the $Nb(Al)_{ss}$ to the A15 phase produces a rapid local heating and propagation of the reaction along the length of the strand. As the self heating is localized to the A15 volume the heat is quickly dissipated after reaction across the Nb and stabilizer volumes so that external Cu stabilizer applied after the initial RQH process is not melted. A further anneal at $\sim$800 °C then provides long range ordering to the A15 phase.

In this paper we step back in magnification from the excellent high resolution TEM work of Kikuchi *et al.* [4] and use a Field Emission Scanning Electron Microscope, FESEM to look at macroscopic variations in the microchemistry and microstructure of Nb_3Al wires and tapes in the RQ untransformed, RHQT and TRUQ conditions. We have previously shown that the FESEM can be used to probe sub-micron variations in Nb_3Sn chemistry by backscattered electron imaging, BEI, [9] and can be used to make accurate measurements of Nb_3Sn grain size using fractured cross-sections for strands with average grain sizes as small as 57 nm in diameter [10]. FESEM has advantages over TEM in ease of specimen preparation and that large areas can be selectively examined with spatial resolutions as high as 4 nm.

Manuscript received August 6, 2002. This work was supported in part by the U.S. Department of Energy under Grant DE-FG02-91ER40643.

P. J. Lee and A. A. Squitieri are with the Applied Superconductivity Center at the University of Wisconsin-Madison, Madison, WI 53706 USA (e-mail: peterlee@wisc.edu).

D. C. Larbalestier is with the Applied Superconductivity Center at the University of Wisconsin-Madison, Madison, WI 53706 USA and is also with the Materials Science Program at the University of Wisconsin-Madison.

T. Takeuchi, N. Banno, T. Fukuzaki, and H. Wada are with the National Institute for Materials Science, Tsukuba 305-0003, Japan (e-mail: TAKEUCHI.Takao@nims.go.jp).

Digital Object Identifier 10.1109/TASC.2003.812334

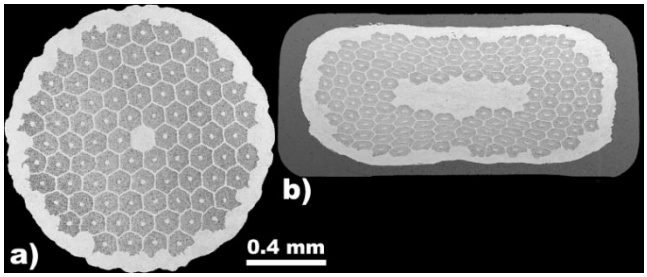

Fig. 1. FESEM-BEI images of transverse cross-sections of as-quenched untransformed composites in (a) un-clad wire form and (b) as processed to Cu-clad tape.

II. Experimental Procedure

A. Strand Fabrication

The precursor Nb/Al multifilamentary composites (Hitachi Cable, Ltd.) were manufactured by the jelly-roll process and cold drawn until the Al laminate size was a few hundred nanometers. The 1.27 mm diameter strand was reel-to-reel ohmically heated to ~1900 °C and quenched to ~50 °C to obtain bcc supersaturated solid solution [$Nb(Al)_{ss}$] filaments in a matrix of Nb. This "untransformed" material [Fig. 1(a)] provided the basis for additional processing including wire drawing and Cu cladding to produce stabilized tape [Fig. 1(b)]. Conversion to Nb_3Al was performed by either applying a standard RHQT process or by the TRUQ process. In both cases an anneal of 10 hrs (36 kS) at 800 °C was used.

B. Metallography

The fractured cross-section technique used to determine grain size in Nb_3Sn was found to be not applicable to the Nb_3Al as trans-granular fracture was dominant. In place of fractography, FESEM BEI, of polished transverse and longitudinal cross-sections was used to provide both microstructural and microchemical information by varying the accelerating voltage for the incident electrons. In the 7–8 kV range there was found to be a balance between the backscatter yields of the Nb and the Nb_3Al leaving surface orientation contrast that could effectively yield the grain structure using long (>1.2 kS) collection times. In the 15–25 kV range atomic number variations provided the dominant contrast image contrast. The polished cross-section for FESEM were prepared by simply by standard metallographic techniques: The strands are mounted in conducting thermosetting (0.9 kS at 177 °C) resin and polished using grinding wheels and ultrasonic polishing. The surfaces are cleaned using metallographic soap applied with a pressurized spray.

FESEM analysis was performed in a LEO 1530 FESEM capable of 4 nm spatial resolution. Backscattered electron imaging was performed using a Robinson scintillator detector with a <0.003Z atomic number discrimination.

C. D.C. Magnetization

DC magnetization was measured in an Oxford Instruments 14 T Vibrating Sample Magnetometer. 4 mm long samples were cut from the rolled specimens, and mounted with the long axis perpendicular to the applied magnetic field. Measurements were taken over 0->14T->0T loops at 4.20 and 12.00 K ± 25 mK.

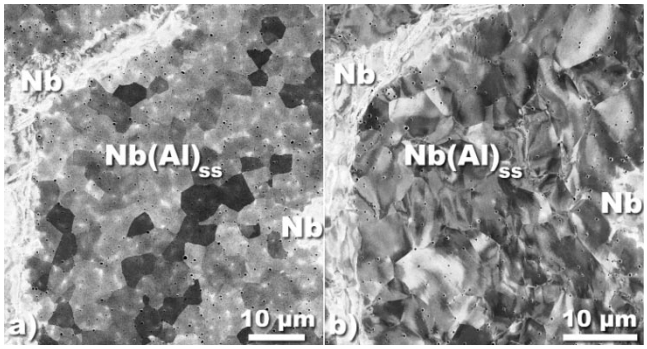

Fig. 2. FESEM-BEI 7 kV images of $Nb(Al)_{ss}$ layers in (a) as-quenched wire at 1.27 mm and (b) after Cu-cladding and forming into tape.

TABLE I
Grain Size (Feret Diameter) and Aspect Ratio of $Nb(Al)_{ss}$ and A15

Wire/Tape	ln-1 mean d*, µm	d*± σ (ln-1), µm	d* mean, µm	mean Aspect Ratio
Wire Untransformed (ME282)	3.08	1.72-5.36	3.47	1.53
Tape Untransformed (ME330)	2.61	1.32-5.16	3.22	1.92
TRUQ Tape (M11-1)	0.93	0.60-1.42	1.01	1.80
RHQT Tape (ME330)	0.98	0.60-1.59	1.10	1.75

d* = Feret Diameter (the diameter assuming grains are circular in cross-section)

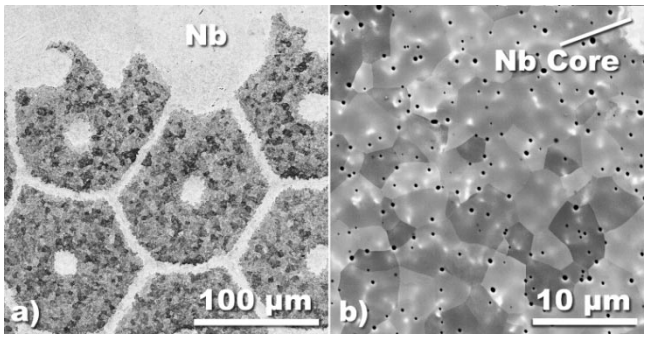

Fig. 3. FESEM BEI atomic number sensitive images at 15 kV of as-quenched, untransformed 1.275 mm diameter wire at (a) low magnification showing distorted edge filaments and (b) at high magnification showing Nb islands and Nb-rich connecting regions as lighter contrast regions.

These were then fit to the Kramer function $J^{1/2} * B^{1/4}$ and B^* estimated from this plot.

III. Results and Discussion

A. Microstructural Quantification

FESEM BEI imaging of the untransformed $Nb(Al)_{ss}$ at 7 kV provided excellent unambiguous determination of grain size [Fig. 2(a)]. After deformation into clad-tape or into reduced diameter strand by wire drawing the contrast was changed to one very similar to TEM of strained samples [Fig. 2(b)] but grain identification was still straightforward. After transformation (both RHQT and TRUQ samples), however, the preponderance of low angle grain boundaries made unambiguous grain determination more difficult. In the FESEM the contrast level between grains increases with the orientation angle between grains whereas the grain boundaries provide direct contrast in TEM. In Table I we compare d^* (the diameter of the grains

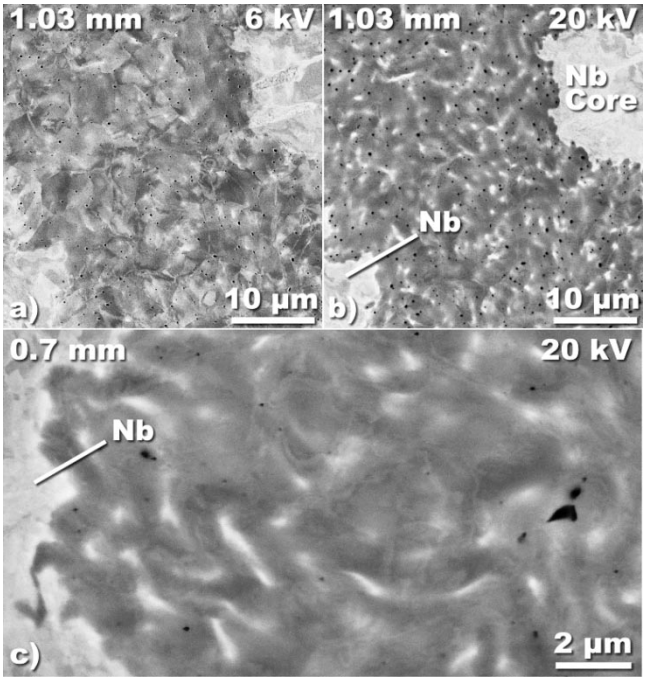

Fig. 4. FESEM BEI images of untransformed quenched and drawn filament layers. (a) low voltage orientation sensitive image of Nb(Al)$_{ss}$ layer. (b) Atomic number sensitive image at 20 kV of the same area. (c) Partial transverse cross-section of an untransformed wire as-quenched and then drawn to 0.7 mm in high voltage atomic number contrast mode. The Nb and Nb-rich regions have been distorted and folded by plane strain deformation of the BCC Nb(Al)$_{ss}$.

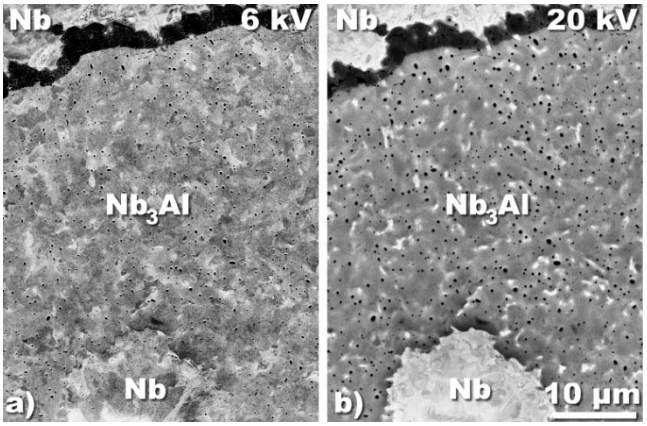

Fig. 5. (a) 6 kV (grain orientation sensitive) and (b) 20 kV (composition sensitive) FESEM BEI images of the same area of an outer filament in a RHQT strand drawn to 1.03 mm diameter. Using a 6 kV accelerating voltage there is very little contrast difference between the Nb (matrix and core) and the Nb(Al)$_{ss}$ and the distortion of the grains produced by the drawing process is noticeable. Using a 20 kV accelerating voltage there is strong compositional contrast between the Nb in the Nb(Al)$_{ss}$ that shows Nb islands as well as lower contrast compositional variation in the Nb(Al)$_{ss}$.

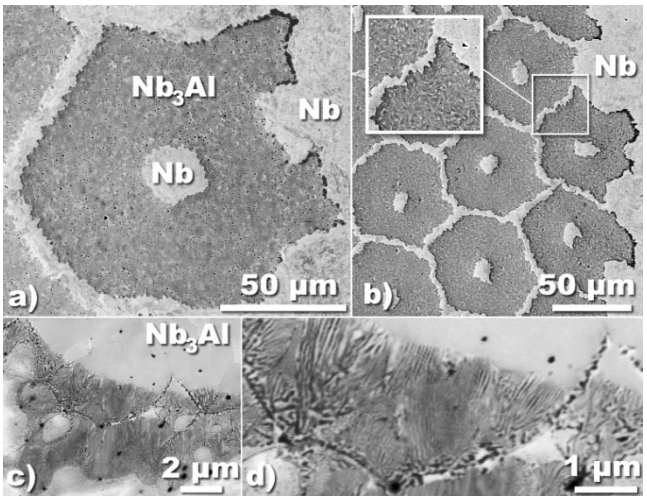

Fig. 6. FESEM-BEI images showing compositional variations in conventionally processed RHQT strand after 10 hr at 800 °C transformation heat treatment. (a) Shows an outer filament at the as-quenched diameter of 1.27 mm (ME282). A high Al, two-phase reaction layer is found on the outer edges closest to the strand edge. Inside voids are distributed nonuniformly. Both high Nb (light contrast) and high Al regions (dark contrast) are clearly visible at this accelerating voltage. (b) Shows the outer filaments of the same composite after being drawn to a strand diameter of 0.7 mm. The swirling nature of the chemical variations can be seen at the higher magnification inset. Additional distortion of the outer filaments is also seen. (c) and (d) show the pearlite type 2-phase reaction layer at the outside edge of the outer filaments (RHQT tape). The closer to the edge of the strand, the thicker the 2-phase layer.

assuming they are circular in cross-section) and aspect ratio for untransformed wire and tape, and TRUQ and RHQT tapes.

As in the cases of Nb_3Sn and Nb–Ti microstructures we find that the distribution in grain diameters is log-normal so we provide both log-normal means and $\pm$ sigma distributions as well as normal means for d^* and aspect ratio for comparison.

The as-quenched untransformed Nb(Al)$_{ss}$ in the 1.275 mm wire has a mean grain Feret diameter of 3 μm (similar to the 2–4 μm reported by Kikuchi *et al.* [4] from TEM analysis. Processed to Cu-clad tape the grain size is reduced and the aspect ratio of the grains increases from 1.53 to 1.92. The aspect ratio for the TRUQ and RHQT Tapes remains high because of the sub-grain structure but the mean grain size is reduced to $\sim$1 μm for the grains and sub-grains with sufficient orientation contrast to be observable by FESEM.

B. Microchemical Analysis

1) Untransformed As Quenched: In Fig. 3 we show a transverse cross-section of the untransformed as quenched 1.27 mm diameter wire imaged in BEI mode with an accelerating voltage of 15 kV in order reveal compositional variations in the filaments. At low magnification, Fig. 3(a), an overall uniform contrast is observed across the filaments independent of location and only showing grain orientations. At high magnification, Fig. 3(b), high atomic number islands with the same atomic number intensity as the Nb core can be observed. The position of the islands ($\sim$300 nm thick and separated by $\sim$4 μm) is independent of the Nb(Al)$_{ss}$ grain structure and the islands are often connected to each other by region of atomic number intensity that are higher that the surrounding Nb(Al)$_{ss}$.

2) Untransformed As Quenched and Drawn: In Fig. 4(a) and (b) we compare a low voltage orientation sensitive image of the Nb(Al)$_{ss}$ layer in an untransformed wire as quenched and drawn from 1.275 mm to 1.03 mm with a high voltage composition sensitive image. In Fig. 4(c) an atomic number sensitive image is shown after further drawing to 0.7 mm. Plane strain deformation of the BCC Nb(Al)$_{ss}$ and Nb during wire drawing

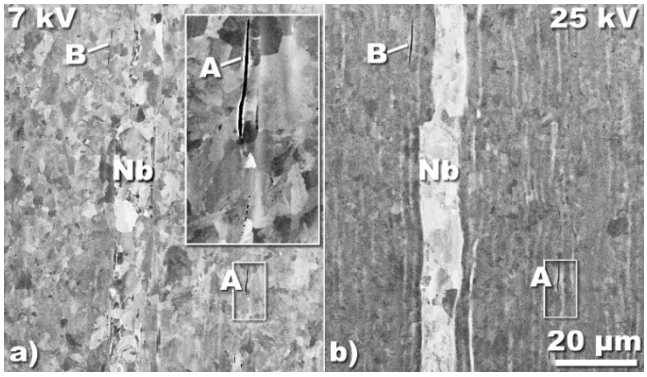

Fig. 7. FESEM BEI images of the same area of a TRUQ tape cross-section at (a) low voltage showing void pipes extending along the tape axis and (b) high voltage showing Nb-rich regions extending along the tape axis.

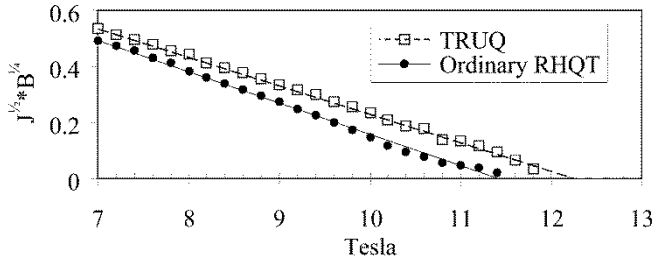

Fig. 8. Comparison of Kramer Plots based on magnetization measurements for TRUQ and Ordinary RHQT tapes at 12 K. TRUQ processed tape has a higher J_c and irreversibility field.

deforms the distorts the grains in transverse cross-section to produce a microstructure after a true strain of only 1.2 (0.7 mm) reminiscent of the production of folded α–Ti ribbons in Nb–Ti based superconductors. In this case, however, the Nb rich regions are 100–200 nm thick and separated by $\sim$1–2 μm. After wire drawing from 1.27 mm to 1.03 mm (true strain of 0.42) the void density is qualitatively similar to that at 1.27 mm diameter, however, after further drawing to 0.7 mm diameter (true strain of 1.2) the void density is much lower [compare Fig. 3(b) with Fig. 4] and some larger distorted voids are visible.

3) Ordinary (RHQT) and TRUQ Wire and Tape: FESEM-BEI imaging of both ordinary RHQT and TRUQ processed strands and tapes indicate compositional inhomogeneity on the same spatial scale as in the untransformed state [Fig. 5 and Fig. 6(a) and (b)]. In addition a pearlite-like eutectic 2-phase reaction layer is produced on the outer surface of the outer filaments [Fig. 6(c) and (d)]. The average composition of the 2-phase region was measured at 90% Al and 10% Nb using EDS. The 1–2 μm spatial resolution of EDS in FESEM is not sufficient to quantify the individual lamellae. The thickness of the layer is very sensitive to position with increasing thickness as the outside of the wire or tape is approached [Fig. 6(b)].

Examined in longitudinal cross-section (Fig. 7) the Nb rich bands extend along the drawing axis. Also void pipes are observed that extend along the drawing axis. The longitudinal observations suggest the inhomogeneity derives from the original jelly-roll Nb sheets in the precursor composite.

4) D.C. Magnetization: The TRUQ process improves the upper critical field at 12 K by approximately 1 T, from a B^* of 11.3 T in the standard process to 12.3 T with the TRUQ (Fig. 8).

IV. Summary

1) FESEM-BEI proves to be a highly useful and efficient tool to probe the microchemistry and microstructure of Nb_3Al composites.
2) Large scale compositional inhomogeneity was observed in untransformed, RHQT and TRUQ wires and tapes. The inhomogeneity extends along the longitudinal axis indicating that it is derived from the original jelly-roll Nb wrap.
3) A 2-phase reaction layer was observed on the RHQT and TRUQ outer filaments and their external faces.
4) A 1 T increase in B^* at 12 T is observed in the TRUQ tape compared to RHQT tape.

References

[1] Y. Iijima, Y. M. Kosuge, T. Takeuchi, and K. Inoue, "Nb_3Al multifilamentary wires continuously fabricated by rapid-quenching," *Adv. Cryog. Eng.*, vol. 42, pp. 1447–1454, 1997.

[2] T. Takeuchi, "Nb_3Al conductors—Rapid-heating, quenching and transformation process," *IEEE Trans. Appl. Superconduct.*, vol. 10, pp. 1016–1021, 2000.

[3] ——, "Nb_3Al conductors for high-field applications," *Supercond. Sci. Technol.*, vol. 13, pp. R101–R119, 2000.

[4] A. Kikuchi, Y. Iijima, and K. Inoue, "Microstructures of rapidly-heated/quenched and transformed Nb_3Al multifilamentary superconducting wires," *IEEE Trans. Appl. Superconduct.*, vol. 11, pp. 3615–3618, 2001.

[5] S. V. Sudareva, N. N. Buynov, and Y. E. P. Romanov, "Observation of shear structures in the compound Nb_3Al," *Fiz. Metal. Metalloved.*, vol. 44, pp. 582–588, 1977.

[6] W. Rong and S. D. Dahlgren, "A microstructural investigation of the bcc to A15 phase transition in sputter-deposited Nb_3Al superconductors," *Metall. Trans. A*, vol. 8, pp. 1763–1768, 1977.

[7] A. Kikuchi, Y. Iijima, and K. Inoue, "Nb_3Al conductor fabricated by DRHQ (Double Rapidly-Heating/Quenching) process," *IEEE Trans. Appl. Supercond.*, vol. 11, pp. 3968–3971, 2001.

[8] T. Takeuchi, N. Banno, T. Fukuzaki, and H. Wada, "Large improvement in high-field critical current densities of Nb_3Al conductors by the transformation-heat-based up-quenching method," *Supercond. Sci. Technol.*, vol. 13, pp. L11–L14, 2000.

[9] P. J. Lee, A. A. Squitieri, and D. C. Larbalestier, "Nb_3Sn: Macrostructure, microstructure, and property comparisons for bronze and internal Sn process strands," *IEEE Trans. Appl. Superconduct.*, vol. 10, no. 1, pp. 979–982, 2000.

[10] L. D. Cooley, A. A. Squitieri, A. Gurevich, A. Johnson, W. Starch, P. J. Lee, and D. C. Larbalestier, "Field and temperature dependence of the critical current density of a PIT Nb_3Sn composite determined by magnetization measurements of tube-shaped reaction layers," *Adv. Cryo. Eng.*, vol. 48B, pp. 925–932, 2002.